Further Studies of the Prompt Neutrons from the Spontaneous Fission of Cf^{252}†

HARRY R. BOWMAN, J. C. D. MILTON,* STANLEY G. THOMPSON, AND WLADYSLAW J. SWIATECKI
Lawrence Radiation Laboratory, University of California, Berkeley, California
(Received 4 October 1962)

Results of neutron and fission fragment time-of-flight measurements on Cf^{252} are presented in detail. The energy spectra and angular distributions of neutrons emitted by pairs of fragments of different degrees of asymmetry and different kinetic energies, as recorded in the laboratory system, have been analyzed for consistency with the hypothesis of isotropic emission from fully accelerated fission fragments.

The center-of-mass energy spectra of the neutrons, when these are assumed to be emitted isotropically from moving fragments, have been found to be representable, within fairly narrow limits, by a standard shape. Given this shape, the neutron distribution may be specified by the number of neutrons ν emitted by a fragment and the average energy $\bar{\eta}$. The two quantities ν and $\bar{\eta}$ have been analyzed as functions of the mass number A of a fragment and the kinetic energy E_K as a fragment pair, and the detailed results are presented in a series of graphs. The variation of ν with A shows the "saw-tooth" dependence found in earlier experiments, which may be studied in greater detail on the basis of our results. In contrast, the dependence of $\bar{\eta}$ on A does not show a discontinuity in the region of symmetrical mass splits, the values of $\bar{\eta}$ being always approximately equal for the two members of a fragment pair.

The results of a few simple calculations are presented along with the data, but no systematic attempt is made to interpret the neutron distributions.

I. INTRODUCTION

IT is the purpose of this paper to discuss in detail the properties of the prompt neutrons associated with the spontaneous fission of Cf^{252}, in particular the number, energy, and angular distribution of the neutrons as a function of the mass and kinetic energy of the fission fragments.

The value of such an exhaustive study is to provide a body of experimental data from which a number of general features of fission may be deduced, and against which theories may be tested both qualitatively and in detail. A by-product of the study has turned out to be an accumulation of information related to the level densities of medium-weight nuclei.

This paper is a continuation of an earlier one[1] in which we discussed the neutron distributions in terms of two major groups of fragments, light and heavy. Except for trivial differences noted in the text, the data are those of reference 1 (referred to hereafter as BTMS). The present paper completes the description of these experimental measurements. As the experimental arrangement and method of taking data were discussed in BTMS, we give only a short resumé here. Briefly, the velocities of both fission fragments were measured in coincidence with a neutron or γ ray as a function of the angle between the direction of the fission fragment and that of the prompt radiation. The latter were detected in two 4-in.-diam by 2-in.-thick plastic phosphors that could be placed at any two of eight positions between 11.25 and 90 deg in increments of 11.25 deg. The Cf^{252} source mounted in the center of the apparatus (see BTMS) was essentially a weightless one of strength 1.5×10^6 fissions/min. It was prepared by the self-transfer method on a backing of 90-μg/cm^2 nickel foil. When a coincidence occurred, the flight time of the neutron or γ ray to one of the detectors, or more rarely both, was recorded along with the flight times of the two fission fragments. All flight paths were roughly a meter long. Provided that none of the γ rays are emitted with a delay time in the range approximately 10 to 10^2 nsec, the distinction between gammas and neutrons can be made rigorously on the basis of their flight times. Gamma rays of lifetimes in this range would be confused with neutrons in this experiment in a rather complicated way, varying with the angle of the detector.

In all, about 250 000 events were studied. About half of all the data is common with the angle 11.25 deg (see BTMS).

II. ANALYSIS OF THE DATA

Discussion of the data falls into two parts. The first concerns the demonstration that the energy and angular distribution of the neutrons is, by and large, consistent with the hypothesis of isotropic evaporation from moving fragments, not only when average fragments of average energy are considered (as in BTMS), but also when different groups of fragments with high or low kinetic energies and high or low mass ratios are examined separately.

The second part concerns the properties of the neutrons (as regards numbers and energies) as functions of the two variables specifying a fission event in our experiment, namely, the mass division and the kinetic energy release for a given pair of fragments. This discussion is presented as follows: The simplifying feature that the data are approximately consistent with the assumption of isotropic evaporation from moving fragments allows one to characterize broadly the neutrons associated with a given pair of fission fragments by just four quantities, two for each fragment: the number and the average energy (or average temperature) of the

† This work was done under the auspices of the U. S. Atomic Energy Commission.
* On leave from Atomic Energy of Canada, Limited, Chalk River, Ontario.
[1] H. R. Bowman, S. G. Thompson, J. C. D. Milton, and W. J. Swiatecki, Phys. Rev. **126**, 2120 (1962).

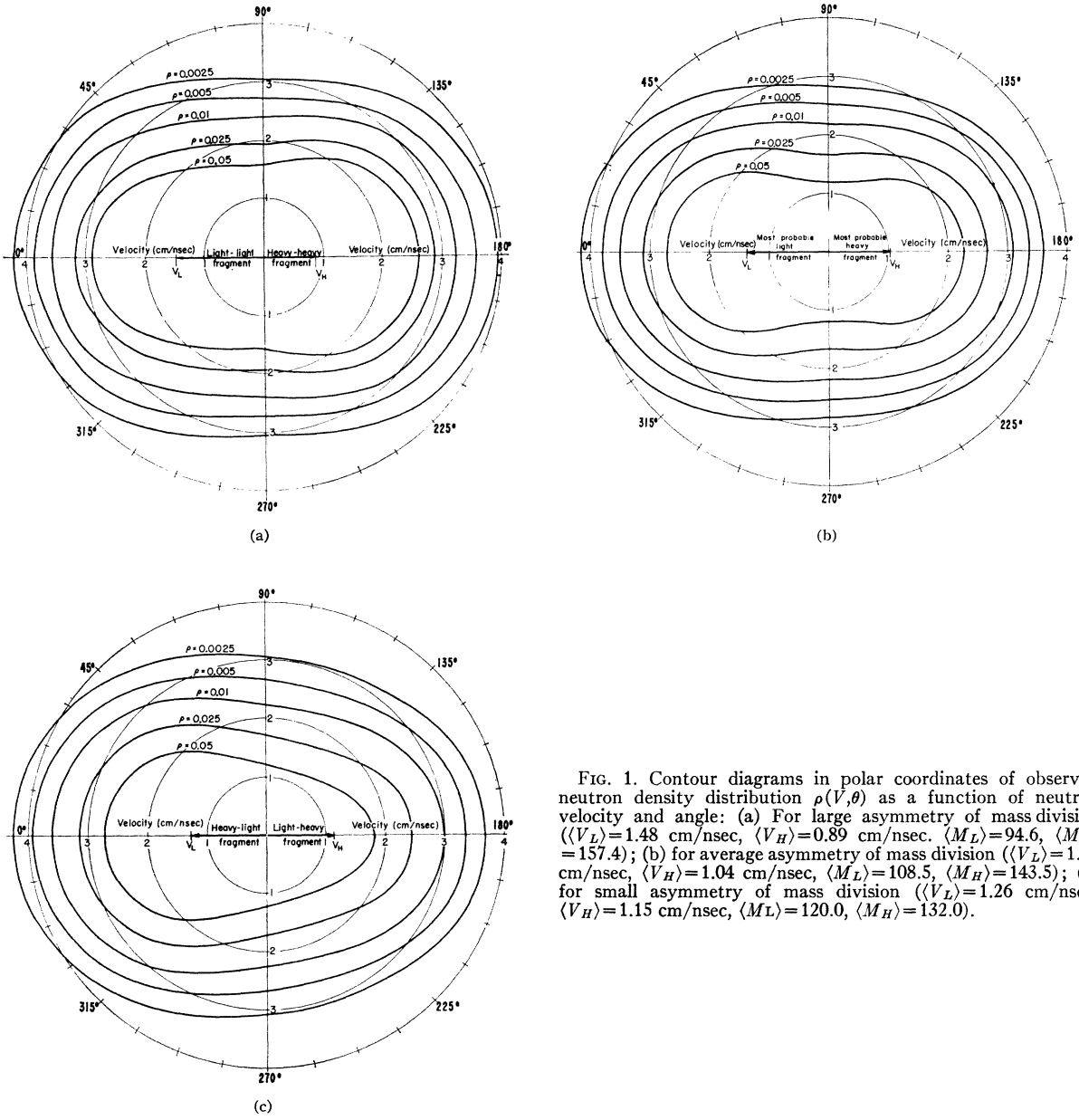

FIG. 1. Contour diagrams in polar coordinates of observed neutron density distribution $\rho(V,\theta)$ as a function of neutron velocity and angle: (a) For large asymmetry of mass division ($\langle V_L\rangle=1.48$ cm/nsec, $\langle V_H\rangle=0.89$ cm/nsec. $\langle M_L\rangle=94.6$, $\langle M_H\rangle=157.4$); (b) for average asymmetry of mass division ($\langle V_L\rangle=1.37$ cm/nsec, $\langle V_H\rangle=1.04$ cm/nsec, $\langle M_L\rangle=108.5$, $\langle M_H\rangle=143.5$); (c) for small asymmetry of mass division ($\langle V_L\rangle=1.26$ cm/nsec, $\langle V_H\rangle=1.15$ cm/nsec, $\langle M\text{L}\rangle=120.0$, $\langle M_H\rangle=132.0$).

neutrons emitted by the light fragment and the corresponding pair of quantities for neutrons emitted by the heavy fragment. When the number of neutrons and their average temperature are considered as functions of the mass division and of the kinetic energy of a fission event, the characteristics of the neutrons may be discussed in terms of two functions of two variables:

(a) Number of neutrons $\nu(A,E_k)$ as a function of the mass A of the emitting fragment and the kinetic energy E_k of the fission event.

(b) Average energy $\bar{\eta}(A,E_k)$ as a function of the mass of the fragment and the kinetic energy of the fission event.

The two quantities ν and $\bar{\eta}$ may be regarded as the zeroth and second moments of the velocity spectrum of the emitted neutrons. In order to specify the velocity spectrum completely, all the other moments would, in principle, have to be determined. One result of this experiment has turned out to be the virtual constancy of the intrinsic *shape* of the spectrum over a fairly wide range of excitations and masses of emitting fragments. The existence of such a standard shape of the evaporation cascade spectrum implies that two numbers are, in fact, sufficient to specify the spectrum: the total number of neutrons ν and one other moment of the distribution, for example $\bar{\eta}$.

A. Hypothesis of Isotropic Evaporation from Moving Fragments

A simple test of the hypothesis of isotropic evaporation from moving fragments was described in BTMS, and we apply this to the different groups of fission events considered in this paper. The test consists of a graphical construction applied to the angular and velocity distribution of the neutrons in the laboratory system as displayed in a contour plot of the "neutron density" $\rho(V,\theta)$ [see BTMS for a discussion of the graphical construction and density $\rho(V,\theta)$]. As remarked in BTMS, the function $\rho(V,\theta)$ is proportional to the density in space of the neutrons that would be found at time t around a source of fission events set off at time zero with the fragments aligned in the same direction in space.

Figures 1(a), (b), (c) show three contour maps of $\rho(V,\theta)$, corresponding to a selection of fission events with exceptionally large asymmetry of mass division, average asymmetry, and small asymmetry, respectively. An examination of these figures shows that although the relative number of neutrons emitted by the two groups of fragments is changing drastically as a function of asymmetry, the $\rho(V,\theta)$ contours remain consistent within 10 to 20% with isotropic evaporation of neutrons from moving fragments.

Plots of $\rho(V,\theta)$ corresponding to selections of combina-

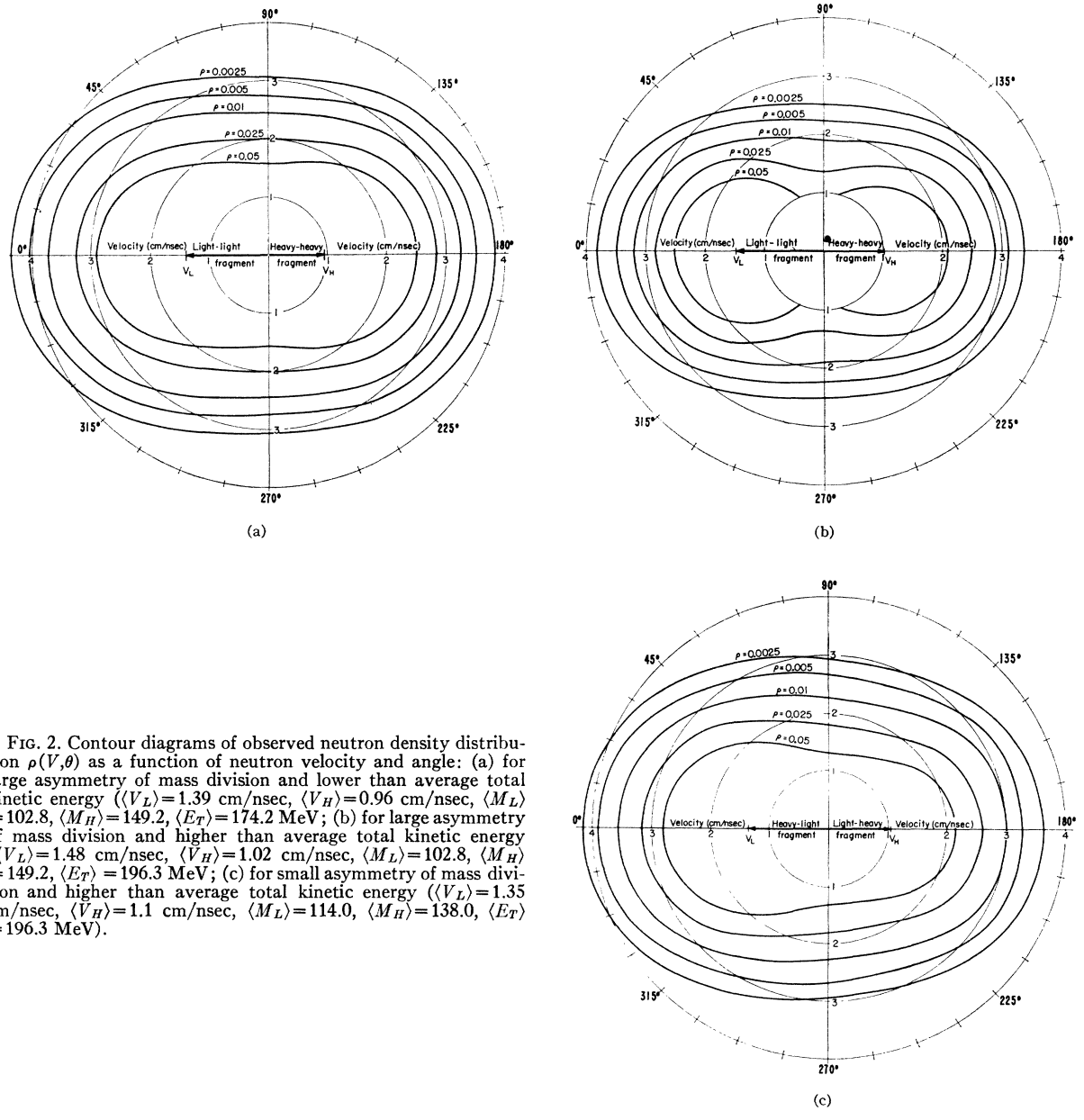

FIG. 2. Contour diagrams of observed neutron density distribution $\rho(V,\theta)$ as a function of neutron velocity and angle: (a) for large asymmetry of mass division and lower than average total kinetic energy ($\langle V_L\rangle=1.39$ cm/nsec, $\langle V_H\rangle=0.96$ cm/nsec, $\langle M_L\rangle=102.8$, $\langle M_H\rangle=149.2$, $\langle E_T\rangle=174.2$ MeV; (b) for large asymmetry of mass division and higher than average total kinetic energy ($\langle V_L\rangle=1.48$ cm/nsec, $\langle V_H\rangle=1.02$ cm/nsec, $\langle M_L\rangle=102.8$, $\langle M_H\rangle=149.2$, $\langle E_T\rangle=196.3$ MeV; (c) for small asymmetry of mass division and higher than average total kinetic energy ($\langle V_L\rangle=1.35$ cm/nsec, $\langle V_H\rangle=1.1$ cm/nsec, $\langle M_L\rangle=114.0$, $\langle M_H\rangle=138.0$, $\langle E_T\rangle=196.3$ MeV).

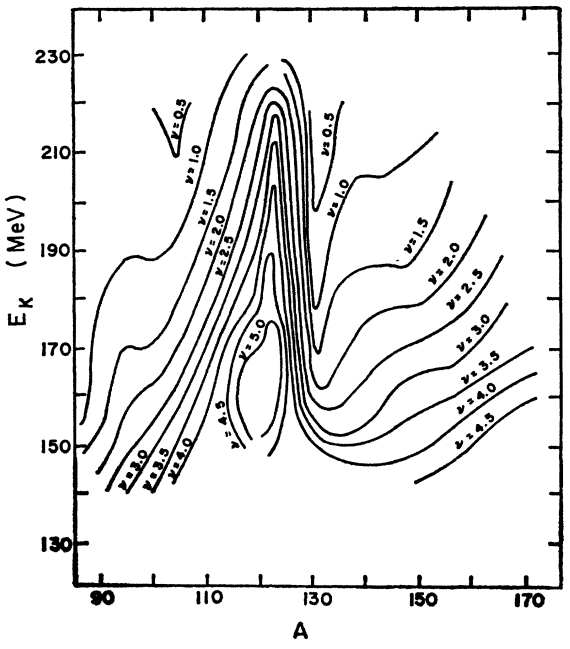

(a)

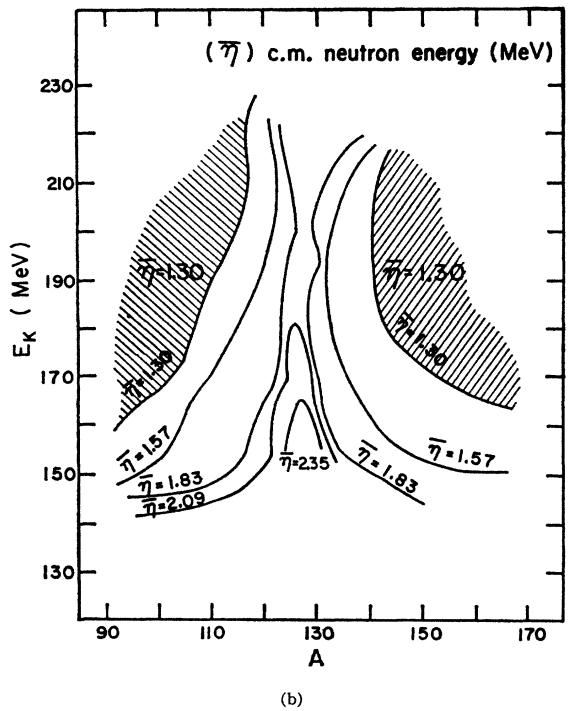

(b)

FIG. 3. (a) Contour diagram of the number of neutrons per fragment as a function of fragment mass A and total kinetic energy E_K. The contour lines are lines of constant number of neutrons (uncorrected for dispersion). (b) Contour diagram of the center-of-mass neutron kinetic energy $\bar{\eta}$ as a function of fission fragment mass A and total kinetic energy E_K. The contour lines are lines of constant neutron kinetic energy. ($\bar{\eta}$ is constant over shaded areas.)

tions of different asymmetries and kinetic energies are shown in Figs. 2(a), (b), (c). Again no large deviations because of isotropic evaporation from moving fragments are revealed. Small deviations can be discerned in a more detailed examination of all $\rho(V,\theta)$ diagrams. Such deviations were discussed in BTMS with reference to fission events of average asymmetry and average kinetic energy. The results of this paper are taken to indicate that no special broad groups of fragments, with selected asymmetries and kinetic energies, are responsible for these deviations.

In view of uncertainties still existing as to the interpretation of these deviations, some of which were discussed in BTMS, we must conclude that although the results of this paper have confirmed in an approximate sense the hypothesis of isotropic evaporation of neutrons as applied to different groups of fission fragments, the delimitation of the extent of the validity of the hypothesis and the determination of the nature of the deviations remain poorly defined.

Since the deviations appear in any case to be small, we can continue our discussion of the data with the simplifying assumption of isotropic evaporation.

B. Methods for Deducing the Center-of-Mass Spectra of the Neutrons

Even with the assumption of isotropic evaporation from fragments, the problem of deducing the center-of-mass spectrum of the neutrons (emitted by each fragment) from the observed laboratory-system distributions is not straightforward, because at each laboratory-system angle only the sum of contributions from the two fragments is observed. Thus, in estimating the number and energy spectrum of the neutrons from one fragment, one must subtract an initially unknown contribution from the other.

In BTMS a direct method of analyzing the neutron distributions was described in which least-squares fits to the data were made by using superpositions of analytical evaporation spectra with several adjustable parameters. This method, if applied to data analysis in this paper, consisting of many groups of fragment asymmetries and energies, would require hundreds of least-squares fits to be made.

A simpler though less direct method is possible, since the perturbation of the neutron spectrum of one fragment by the other is not large on the average and may be treated as a correction. The situation is actually complex in the sense that at certain laboratory-system angles (near 90 deg to the fission direction) the perturbation is large (both fragments contributing about equally), whereas at other angles (near 0 deg) the perturbation is negligible, since very few neutrons from the fragment moving away from the neutron counter have sufficiently high velocities to perturb the distribution of the neutrons from the fragment moving toward the neutron counter.

The complexity of the effect, making the perturbation small at certain angles and large at others, has led us to two—partly independent—ways of analyzing the data. In the first, only the "small-angle" data from 11.25 and 168.75 deg were analyzed. Here the corrections discussed above can be considered negligible, but about half the data are discarded. In the second method, data from all angles are used, but subject to large corrections.

Both methods were tried in some of the analyses, but after essential agreement between the two methods had been found (confirming incidentally that the hypothesis of isotropic emission was not seriously wrong), most of the detailed studies discussed below were made with the aid of the more straightforward small-angle method. (An added advantage of this method is that because of the fragment's velocity in the direction of the counter at 11.25 or 168.75 deg, even neutrons leaving a fragment with almost vanishing velocity arrive at the detector with an energy at which the detection efficiency is good.)

In the first method, the procedure was to calculate for every event the c.m. neutron velocity v from the observed laboratory velocity V and the fragment velocity V_F. From the distribution of the recorded values of v the nth moment of the c.m. spectrum of the neutrons could then be calculated by using the general formula given in Appendix A.

In the second method, the zeroth and second moments of the c.m. neutron spectra were calculated by assuming, first, that all the neutrons observed at angles between

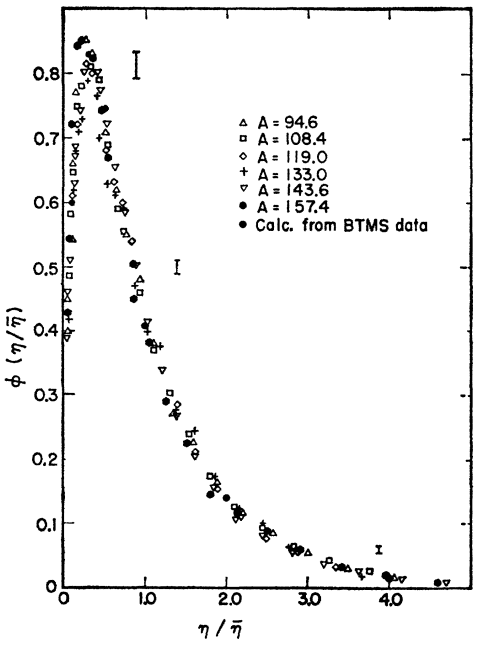

FIG. 4. The center-of-mass neutron energy distribution normalized to integrate to unity and expressed in dimensionless units $(\eta/\bar{\eta})$. Data (uncorrected for dispersion) for six different fragment masses are plotted. (No selection in E_K.)

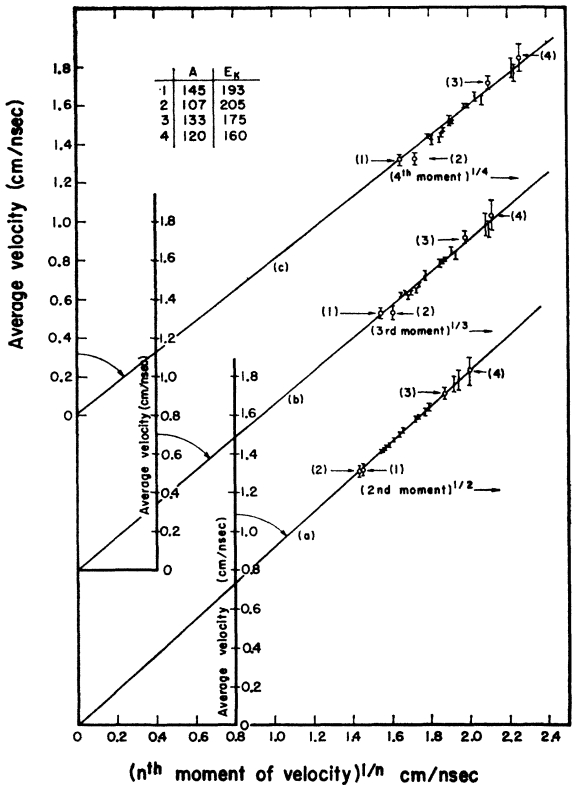

FIG. 5. The relation of the first moment of the center-of-mass velocity distributions to the higher moments of the velocities (a) the first vs the square root of the second, (b) the first vs the cube root of the third, (c) the first vs the fourth root of the fourth moment. The unlabeled points correspond to different fragment masses ranging from $A \approx 85$ to $A \approx 165$, with no selection in the kinetic energy E_K. The effect of selecting kinetic energies as well as masses is shown by the labeled points (uncorrected for dispersion).

0 and 90 deg were associated with the light fragment, and all neutrons observed between 90 and 180 deg were associated with the heavy fragment—or, equivalently, that as many neutrons from the light fragment went into the "heavy fragment hemisphere" ($\theta > 90$ deg) as there were neutrons from the heavy fragment that went into the "light fragment hemisphere" ($\theta < 90$ deg). A correction was then applied for the approximate nature of this assumption (see Appendix B for details).

III. RESULTS

A. Tabulation of the Data

The results of the analyses described above are shown in a series of figures designed to bring out different aspects of the manifold distributions. Figure 3(a) gives a compact contour plot of the zeroth moment—the number of neutrons per fragment—as a function of A and E_K. It may be seen from this plot that the number of neutrons emitted by a fragment of a given mass increases roughly linearly with decreasing kinetic energy of the fission event. On the other hand, the dependence

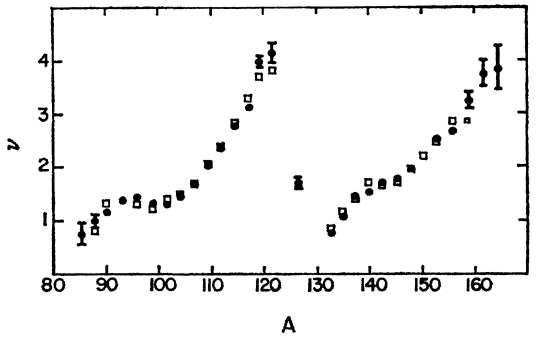

FIG. 6. The variation of the number of neutrons per fragment with fragments mass. The circles correspond to data taken at small angles from the direction of motion of the fragments. The squares correspond to data taken at all angles. (Corrected for resolution.)

on fragment mass at a given kinetic energy is not simple, with rather violent changes in the number of neutrons near mass 130 (which also happens to be near symmetry for Cf^{252}). It is especially worth noting that even at low kinetic energy releases, or high total excitation energies, there are very few neutrons associated with masses near 130. Figure 3(b) gives a contour plot similar to Fig. 3(a), but in this instance for the average c.m. neutron energy $\bar{\eta}(A,E_K)$. The variation of $\bar{\eta}$ with mass is less drastic than was the case for ν, and the pattern of the contours of constant $\bar{\eta}$ is approximately symmetrical about mass 126.

B. Existence of a Standard Shape of the Evaporation Cascade Spectrum

As remarked in Sec. II, the average values of ν and $\bar{\eta}$ would be sufficient to specify the velocity distributions of the neutrons if a standard intrinsic *shape* could be assumed for the velocity spectra. The extent to which this is the case, over the range of excitation energies and masses considered in this experiment, is illustrated in Fig. 4. The c.m. spectra in this figure were deduced from the "small-angle data." The observed spectra have been normalized to integrate to a total number of neutrons of unity. The energy is expressed in dimensionless units

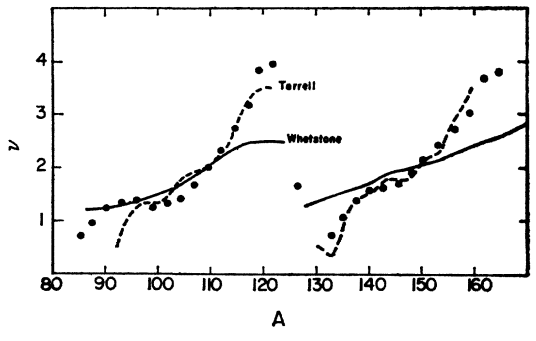

FIG. 7. The variation of the number of neutrons per fragment with fragment mass. Our measurements (circles) are compared with the results of (a) Whetstone (reference 3) (solid line) and (b) those deduced by Terrell (reference 5) (broken line).

by dividing through by the average energy of the distribution in question. We note that only small deviations from a standard shape are apparent. A plot on a logarithmic scale exhibits some of the deviations in the tails of the spectra which, however, are less well determined experimentally.

A more compact way to study the hypothesis of a standard shape of the evaporation cascade spectra is to examine the various distribution moments. For a standard intrinsic shape, all higher moments should be deducible from the first: For example, the ratio of the nth root of the nth moment $\langle v^n\rangle^{1/n}$ to the first moment $\langle v^1\rangle$ should be a constant, and a plot of $\langle v^1\rangle$ vs $\langle v^n\rangle^{1/n}$ should fall on a straight line through the origin. Such plots, including up to the fourth moment, are illustrated in Fig. 5. We see that the data from rather different conditions of emission appear to satisfy this test for a standard shape rather well. The neutron spectra discussed in BTMS (for average light- and heavy-fragment

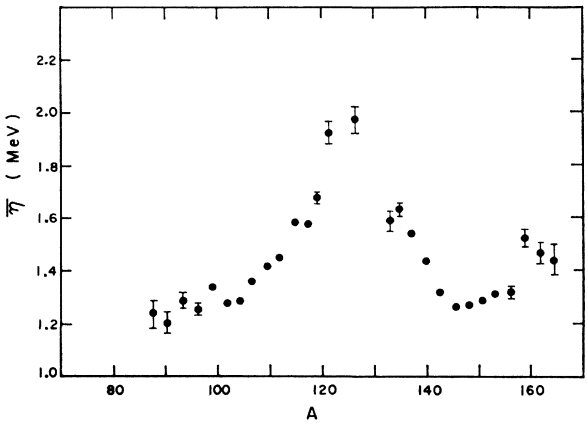

FIG. 8. The average center-of-mass neutron kinetic energy as a function of fragment mass, corrected for mass resolution.

groups) are also consistent with the standard shape in Fig. 4, as they should be, since they represent certain averages of the data there. The analysis of those shapes in terms of superpositions of evaporation spectra enables us to write down an analytical formula for the shape $\phi(\eta/\bar{\eta})$ in Fig. 4. Using the set of three temperatures and weights corresponding to line 8 of Table 6 in BTMS—i.e., $T_1=0.9266$, $T_2=0.3311$, $T_3=0.0461$; and $\alpha_1=0.6112$, $\alpha_2=0.3790$, and $\alpha_3=0.0098$—we find

$$\phi(x)=1.365x\exp(-x/0.669)+6.63x\exp(-x/0.239)+8.8x\exp(-x/0.033),$$

where x stands for $\eta/\bar{\eta}$. Note that $\int_0^\infty\phi(x)dx=1$, and $\int_0^\infty x\phi(x)dx=1$.

To illustrate the use of this formula, suppose we are given that, in an evaporation cascade, an average of 2.9 neutrons were emitted with an average energy of 1.4 MeV. Then the number of neutrons with energies between η and $\eta+d\eta$ predicted by our formula would

be given by

$$2.9\phi(\eta/1.4)d(\eta/1.4).$$

It would be interesting to investigate the extent of the validity of the standard shape $\phi(x)$ in evaporation cascades other than those following from the de-excitation of fission fragments and in the case of the fission of nuclei other than Cf^{252}.

C. Neutron Number and Energy as a Function of Fragment Mass

One of the more interesting facts concerning fission neutron emission is the variation of the average number of neutrons per fragment, $\nu(A)$, with the mass of the fragment. The results of experiments[2–4] on this topic have been recently well summarized by Terrell.[5] We present here a new measurement of greater statistical accuracy than previous ones, and also give the average energy and width of the neutron spectra associated with the fragments.

The new results on the variation of ν with fragment mass are shown in Fig. 6. It can be seen that the two methods of analyzing the data discussed in the preceding section are in excellent agreement. Although the small-angle data are included in the "all-angle" data, they receive relatively little weight because of the $\sin\theta$ factors. The dominant angle in this set is, in fact, 90 deg. The data presented in Fig. 6 have been corrected for mass resolution in addition to the corrections already discussed. The method of unfolding the mass resolution is that suggested by Terrell.[5] Its application here is discussed in Appendix C.

Our data differ from those previously reported[3] in three respects. First, the variation of ν with mass is much greater than in the earlier experiments. As many as four neutrons are emitted on the average from mass 120, whereas in all likelihood fewer than one is emitted by masses near 132 and 85. Second, in addition to the fairly steady increase in ν in going through each mass peak, there appears to be a leveling off in the region of the most probable yields. In fact, there is even a statistically significant peak at about mass 95. Finally, the average number of neutrons from the light fragment is about 20% greater than from the heavy. This difference is more accurately found as $\nu_L/\nu_H=1.17\pm0.03$ in BTMS.

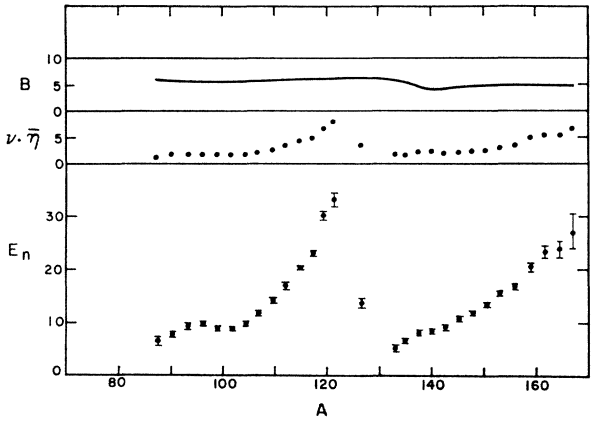

FIG. 9. The average excitation energy E_n, appearing in the form of prompt neutrons, as a function of mass. The neutron-binding energies B and average kinetic energies $\nu\bar{\eta}$ are shown in the upper part of the figure.

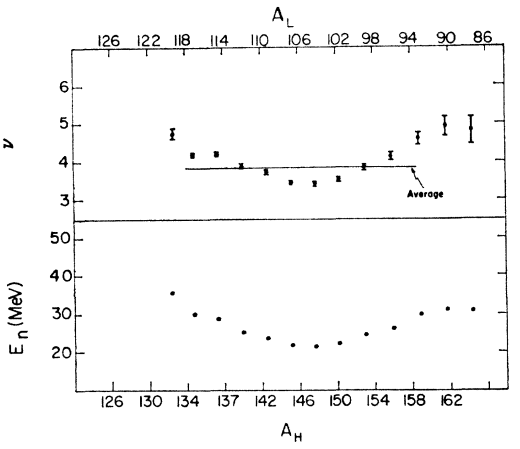

FIG. 10. Total number of neutrons per fission ν and total energy E_n in the form of prompt neutrons as a function of mass pairs.

In Fig. 7 we compare our results with those found by Whetstone[3] by using a high-efficiency neutron detector, and those deduced by Terrell[5] from a comparison of prompt mass yields and final chain yields. The agreement with Terrell's values is excellent, even though he quotes a rather large error.

A new quantity found in the present work is the average c.m. neutron kinetic energy $\bar{\eta}$ as a function of fragment mass (Fig. 8). From these values, together with the values for ν from Fig. 6 and the neutron binding energies calculated by Milton,[6] we are able to find that part of the excitation energy which is carried away by neutrons. The result is shown in Fig. 9 for the individual fragments, while the total on both fragments of a pair is shown in Fig. 10. Thus, we see that although the excitation energy E_n vaires a great deal for single fragments, the total excitation for both fragments is more nearly uniform, showing a shallow minimum near the most probable mass division.

Figure 11 shows plots of ν vs fragment mass for several values of the total kinetic energy release. It is clear that a basic saw-toothed distribution of the excitation energy exists that persists even when the kinetic energy release is low, in which case the total final excitation energy of

[2] J. S. Fraser and J. C. D. Milton, Phys. Rev. **93**, 818 (1954).
[3] S. L. Whetstone, Phys. Rev. **114**, 581 (1959).
[4] V. F. Apalin, V. P. Dobrynin, V. P. Zkharova, I. E. Kutikov, and L. A. Mikaelyan, At. Energ. (U.S.S.R.) **8**, 15 (1960).
[5] James Terrell, Phys. Rev. (to be published).
[6] J. C. D. Milton, University of California Radiation Laboratory Report UCRL-9883-rev. (unpublished).

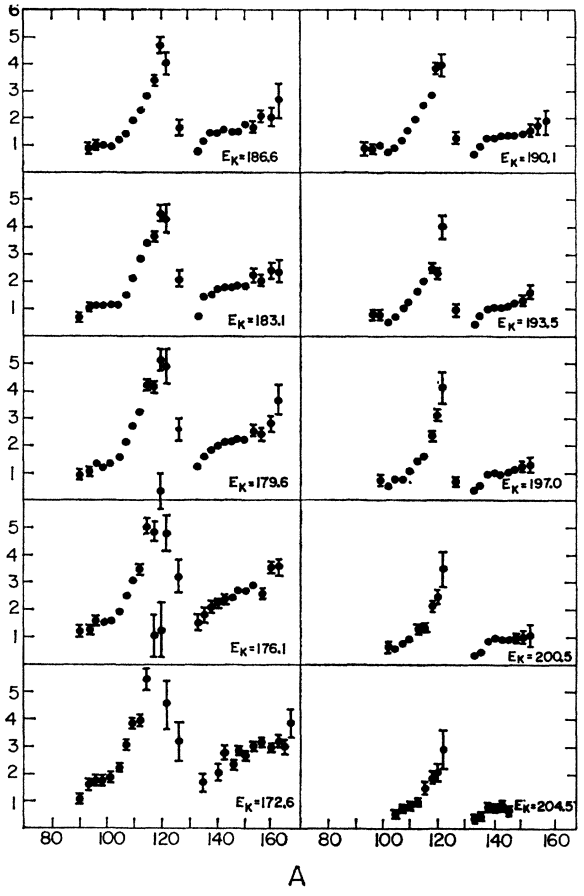

FIG. 11. Average number of neutrons per fragment ν as a function of fragment mass, for selected total kinetic energy intervals.

the fragments E_x is around 40 or 50 MeV. Estimated excitation energies may be obtained from Table I which contains binding-energy and energy-release data calculated by Milton.[6]

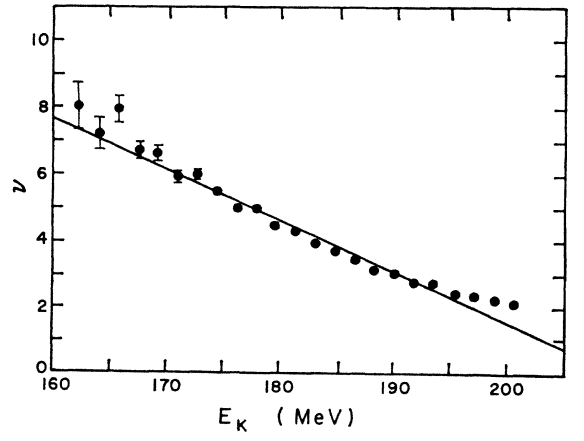

FIG. 12. Variation of the number of neutrons ν with total kinetic energy of fragments. The straight line was drawn to have a slope corresponding to 6.6 MeV/neutron.

TABLE I. Binding energy table for Cf^{252}. The most probable charge, Z_P, is that charge which gives the maximum energy released E_R averaged over the charge distribution. The average neutron binding energies for the light and heavy fragments ($\langle BE_L\rangle_{av}$ and $\langle BE_H\rangle_{av}$) are then found at Z_P by interpolation in the average neutron binding energy tables. The light fragment masses, M_L, are listed on the right and the heavy fragments, M_H, on the left.

M_H	Z_{PH}	$\langle BE_H\rangle_{av}$	E_R	$\langle BE_L\rangle_{av}$	Z_{PL}	M_L
126	49.00	5.869	228.42	5.869	49.00	126
127	49.28	6.185	229.03	6.059	48.72	125
128	49.66	6.264	229.55	5.970	48.34	124
129	49.77	6.099	229.49	5.974	48.23	123
130	50.04	6.417	229.97	6.375	47.96	122
131	50.36	6.107	229.82	6.073	47.64	121
132	50.62	5.736	229.25	6.079	47.38	120
133	51.19	5.704	228.61	6.097	46.81	119
134	51.73	5.445	228.03	5.924	46.27	118
135	52.08	4.728	226.47	5.623	45.92	117
136	52.37	4.368	225.41	5.927	45.63	116
137	52.90	4.291	223.38	5.947	45.10	115
138	53.48	4.277	222.20	5.602	44.52	114
139	53.63	4.083	220.48	5.629	44.37	113
140	53.94	4.184	218.89	5.831	44.06	112
141	54.19	4.027	217.10	5.490	43.81	111
142	54.32	4.211	216.04	5.823	43.68	110
143	54.75	4.405	214.48	5.787	43.25	109
144	55.09	4.382	212.87	5.467	42.91	108
145	55.35	4.641	212.43	5.726	42.65	107
146	55.76	4.799	211.62	5.677	42.24	106
147	55.95	4.614	210.39	5.380	42.05	105
148	56.19	4.867	210.04	5.815	41.81	104
149	56.63	4.878	209.17	5.664	41.37	103
150	56.96	4.686	207.79	5.394	41.04	102
151	57.33	4.942	207.75	5.716	40.67	101
152	57.81	5.065	207.25	5.714	40.19	100
153	58.09	4.773	206.18	5.422	39.91	99
154	58.31	4.917	205.93	5.747	39.69	98
155	58.83	5.041	204.97	5.661	39.17	97
156	59.40	4.966	204.47	5.300	38.60	96
157	59.58	4.860	204.18	5.447	38.42	95
158	59.96	5.054	203.66	5.676	38.04	94
159	60.31	4.782	202.88	5.414	37.69	93
160	60.47	4.734	202.50	5.634	37.53	92
161	61.08	4.988	201.45	5.573	36.92	91
162	61.63	4.950	201.38	5.439	36.37	90
163	61.89	4.680	200.41	5.541	36.11	89
164	62.20	4.903	199.99	5.803	35.80	88
165	62.64	4.870	199.12	5.855	35.36	87
166	63.14	4.736	197.78	5.814	34.86	86
167	63.55	4.872	197.64	6.406	34.45	85
168	64.03	5.117	196.48	6.996	33.97	84
169	64.54	5.018	195.07	6.819	33.46	83
170	64.93	4.843	192.51	6.712	33.07	82

D. Neutron Number and Energy as a Function of Kinetic Energy Release

In Fig. 12 we illustrate the variation of ν with the total kinetic energy E_K. No essentially new features are evident over those found in the earlier work of Stein and Whetstone,[7] who had less statistical accuracy and somewhat poorer energy resolution. Inasmuch as $E_K=E(\text{total})-E_x$, the slope $dE_x/d\nu$ is expected to be the average energy per neutron, and that is what it turns out to be. The value calculated from the weighted average binding energy (5.2 MeV) and the average c.m. neutron kinetic energy (1.4 MeV) is 6.6 MeV, in good

[7] W. E. Stein and S. L. Whetstone, Phys. Rev. **110**, 476 (1958).

agreement with the observations. Unlike the case of the earlier experiment, our data enable us to look at $\nu(E_K)$ for selected masses as shown in Fig. 13, and the picture is not significantly altered. The outstanding feature is the one discussed in the previous section; that is, the division of energy between the fragments near symmetry remains unequal even at high total excitation energies.

A new result of this work is given in the curve of $\bar{\eta}$ versus E_K in Fig. 14. The variation is nearly a straight line of slope $d\bar{\eta}/dE_K = -0.012$. A more detailed presentation of the experimental variation of $\bar{\eta}$ with E_K for selected masses is shown in Fig. 15. The most compre-

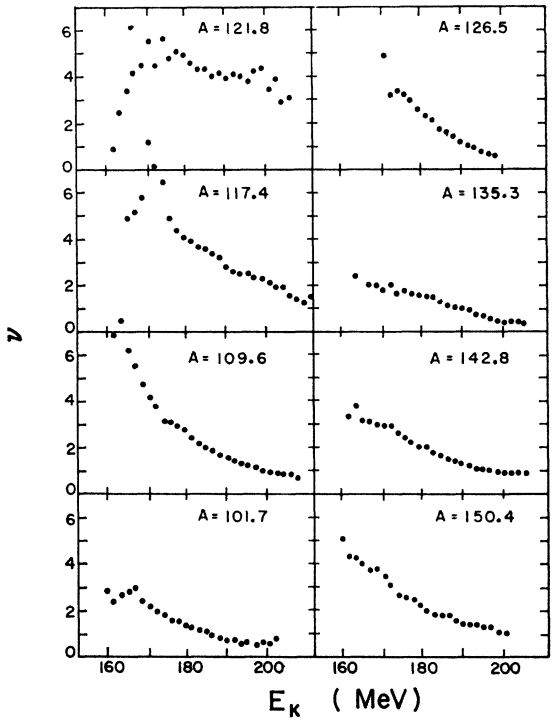

FIG. 13. Number of neutrons ν vs total kinetic energy E_K for selected fragment masses A.

hensive statement of the results of our experiment, with the zeroth, first, and second moments of the c.m. neutron velocities (and their errors) given as functions of fragment mass A and kinetic energy released E_K are printed in tabular form in Lawrence Radiation Laboratory Report UCRL-10139 Rev. (unpublished).

IV. DISCUSSION

The picture that emerges from our analysis of the neutrons emitted in the spontaneous fission of Cf^{252} is a mixture of simplicity and complexity. On the one hand, the simple hypothesis of isotropic evaporation from moving fragments, although not quite accurate within the precision of our experiment, describes the over-all features of the neutrons quite well, even when

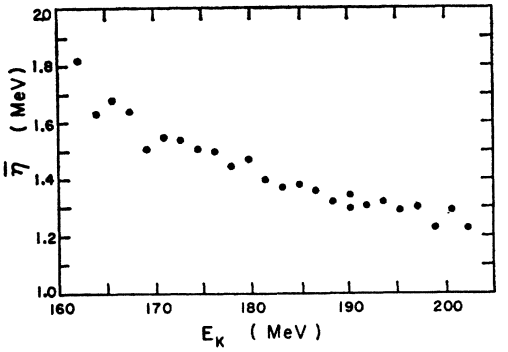

FIG. 14. The relation between the average center-of-mass neutron kinetic energy $\bar{\eta}$ and the fragment total kinetic energy E_K (corrected for resolution).

special groups of fission events are selected. Deviations from isotropic evaporation, which might well have been expected to be appreciable if the breaking up of the neck connecting the fragments had been sufficiently violent, appear instead to be small. An assessment of the significance of this result in placing an upper limit on the violence of the snapping of the neck will require further theoretical studies of this difficult problem. A beginning has been made by Fuller.[8] According to Fuller's esti-

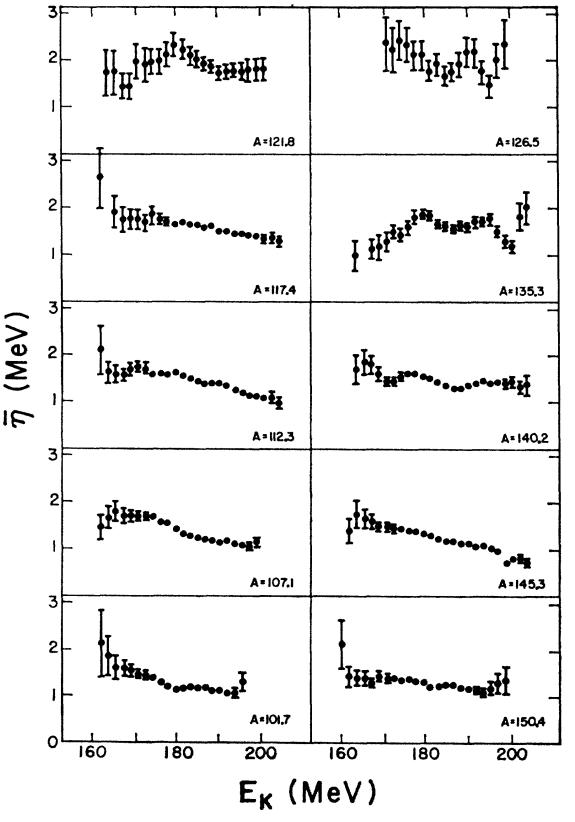

FIG. 15. Average center-of-mass neutron kinetic energy $\bar{\eta}$ vs fragment total kinetic energy E_K for selected masses A.

[8] Robert W. Fuller, Phys. Rev. **126**, 684 (1962).

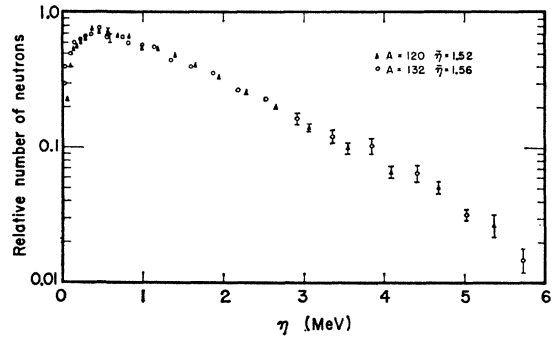

FIG. 16. The relative center-of-mass neutron energy distributions, proportional to $\phi(\eta)$, corresponding to neutrons coming from mass 120 and from mass 132.

mates, a degree of violence of the snapping, described by a complete severance of the neck in 2.5×10^{-22} sec, would result in the ejection of about 1.5 neutrons per fission. Assuming that the angular distribution and energy of such neutrons would not by accident be such as to make them indistinguishable from evaporation neutrons, we could conclude on the basis of his results that the severance of the neck must be more gentle.

Another simplifying feature of our results is the existence of a standard shape of the evaporation cascade spectrum which approximately represents the energy distributions of neutrons emitted under rather different conditions. Again, one might have expected the shape of the spectrum of neutrons emitted by fragments around mass 132, where the average number of neutrons is anomalously low to be different from the case of the profuse emissions around mass 120, but in fact the differences are minor (see Fig. 16).[9]

A further simple feature of our results is the rather smooth decrease of the number and energy of the neutrons as functions of the kinetic energy release for a given fragment mass. The sign and magnitude of the effect is that expected on the basis of primitive estimates.

In contrast to this, the dependence of the neutron number on fragment mass shows a behavior even more violent than was found by Whetstone.[3] Moreover, we find the saw-tooth behavior dominating the dependence of neutron number on fragment mass at all values of the kinetic energy release, i.e., over a range of conditions in which the final excitation of the fragments varies from about 15 to 50 MeV.

In the absence of a quantitative theory of fission, in particular of a theory of the shapes and excitations of fission fragments as functions of mass division, an assessment of the significance of these results is not possible. It has been suggested that the unusually low excitations found around mass numbers 132 and 85 are associated with special features of closed-shell nuclei.[3,10] A discussion of the role of the special stability of closed shells on the deformations to be expected in a pair of interacting fragments is being prepared by two of the authors. In any case, if shell effects in one form or another are invoked to explain the deficiency of neutrons associated with masses around 85 and 132, it would seem necessary to assume, in view of the persistence of the saw tooth even at high final excitations, that at scission the fragments in question are sufficiently cold to allow shell effects to have effect, since at high excitations one would expect them to disappear. An estimate of the temperature at which shell effects disappear may be obtained if assumptions are made about the behavior of nuclear level densities in the neighborhood of closed shells. We illustrate our discussion with the aid of Cameron's rule for level densities.[11] Using Cameron's formula, we calculated how a given amount of excitation energy would be distributed on a pair of Cf^{252} fission fragments assumed to be undistorted and in thermal contact. The result for different total excitation energies from 10 to 40 MeV is shown in Fig. 17. It is seen that at low excitation energies the results are indeed very suggestive of the experimental saw-tooth curve for the excitation energy as a function of mass, but that at excitations sufficiently high to emit four or five neutrons there are hardly any shell effects left. Figure 18 compares the predicted dependence of the average value of ν on A with our measurements. We conclude from this either that shell effects are much more persistent at high temperatures than Cameron's formula suggests, or that the nascent fission fragments are relatively cold at scission, at least for those mass divisions in which closed shells are involved. In the second case, a large part of the energy that later appears as excitation would at scission be bound up in some other form, for example, as potential energy of deformation. This conclusion is also reasonable on other

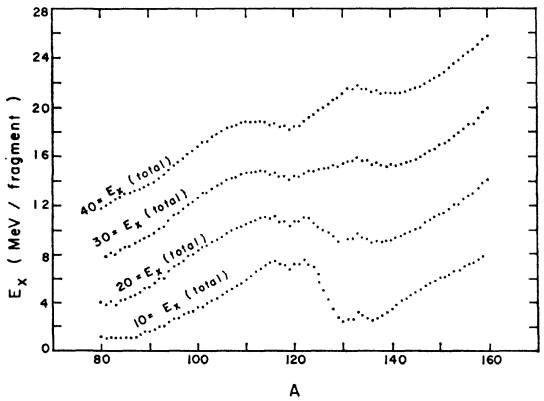

FIG. 17. Calculated excitation energy E_x as a function of fragment mass for different excitation energies E_x (total) of fragment pairs, using Cameron's rule for level densities.

[9] The quite remarkable similarity in the spectra even in these extreme cases is illustrated in Fig. 16, where the two neutron spectra are plotted. The plot is in arbitrary units, but the total numbers of neutrons have been normalized to a common value.

[10] V. V. Vladimirski, Soviet Phys.—JETP **5**, 673 (1957).

[11] A. G. W. Cameron, Can. J. Phys. **36**, 1040 (1958).

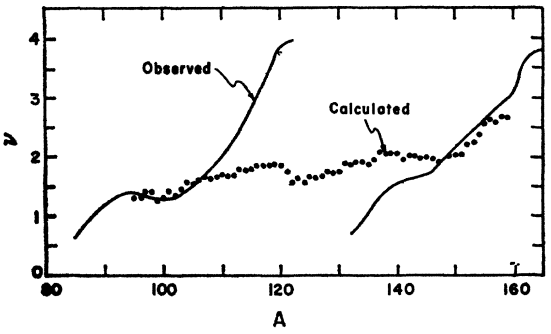

FIG. 18. Predicted variation in the number of neutrons as a function of fragment mass obtained by using Cameron's rule for level densities, compared with observations.

grounds in view of the magnitude of the deformation energy in a pair of interacting fragments, which is suggested by the optimum tangent-spheroid configurations of Cohen and Swiatecki.[12]

If it be true that at scission the Cf^{252} nucleus is essentially cold, calculations based on the statistical equilibrium of hot undeformed fragments in thermal contact, such as those discussed by Newton,[13] Cameron,[14] and more recently Newson,[15] would not apply, at least in the region of shells. An essential feature of the discussion of the conditions prevailing at scission of Cf^{252} would entail a consideration of the deformations of the fragments and of the associated potential energy. An attempt to take into account the deformation energy of fragments at scission has been made in the earlier statistical studies by Fong.[16]

A by-product of our study of the neutrons emitted in Cf fission is the information related to level densities of fragment nuclei of different masses contained in the relationship, for a given nucleus, between the number of evaporated neutrons ν and their average energy $\bar{\eta}$. The number ν being related to the initial excitation energy, and the average energy $\bar{\eta}$ to the average temperature of the nucleus during the de-excitation, we have in effect an implicit relationship between energy and temperature, and thus a possibility of studying the level densities of various nuclei. Data of the type that we have obtained contain a considerable amount of information on level densities which could be extracted by adequate treatment of the de-excitation process. We do not attempt such an analysis in this paper, but limit ourselves to pointing out a few striking features of the results.

A comparison of the experimental functions $\nu(A)$ and $\bar{\eta}(A)$ shown in Figs. 6 and 8 reveals the surprising fact that whereas the saw-tooth function $\nu(a)$ is very asymmetric with respect to mass 126, the energy $\bar{\eta}(A)$ is nearly symmetric. In particular, fragments around mass 120, emitting an average four neutrons, and fragments around mass 132, which emit fewer than one, nevertheless evaporate their neutrons with similar energy spectra and very nearly equal average energies.

The similarity of the energy spectra of neutrons produced under dissimilar circumstances has already been noted in BTMS with reference to spectra from average light and heavy groups of fragments, where the difference in the average values of ν was, however, only 17%. The present results show that the spectra of neutrons from a pair of fragments are similar even when the excitation energies differ by *several hundred percent.* Moreover, this similarity extends over all conditions of total excitation, as seen from the approximate symmetry of all the curves in Fig. 19.

If the near equality of the average energies of the neutrons is taken as evidence for the near equality of the effective temperatures of pairs of fragments during the evaporation of the neutrons, we are led to ascribe very different heat capacities to fragments around mass 120 and those around mass 132; the ratios of excitation energies necessary to produce the same temperature in the two regions are of the order of 4 to 1, or more. A plot that brings out this difference is shown in Fig. 20, where the square root of the excitation energy per particle is compared with the average energy of the emitted neutrons for different masses. For a simple evaporation process governed by a temperature proportional to the square root of the excitation energy per

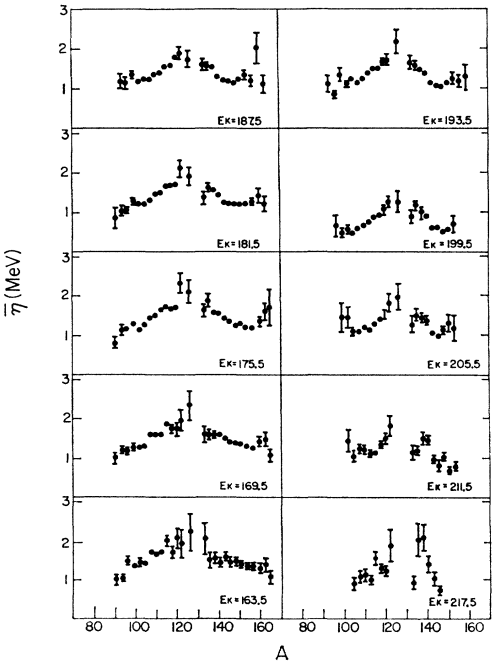

FIG. 19. The average center-of-mass neutron kinetic energy $\bar{\eta}$ as a function of mass, corresponding to selected total kinetic energies of fragments E_K.

[12] S. Cohen and W. J. Swiatecki, Ann. Phys. (N.Y.) (to be published).

[13] T. D. Newton, Atomic Energy of Canada Ltd., Chalk River Project Report AECL-329 1956 (unpublished).

[14] A. G. W. Cameron, in *Proceedings of the Second United Nations International Conference on the Peaceful Uses of Atomic Energy, Geneva, 1958* (United Nations, Geneva, 1958), Paper A/Conf. 15/9/198; also see Atomic Energy of Canada Ltd., Chalk River Project Report AECL-608 (1958) (unpublished).

[15] H. W. Newson, Phys. Rev. **122**, 1224 (1961).

[16] Peter Fong, Phys. Rev. **102**, 434 (1956).

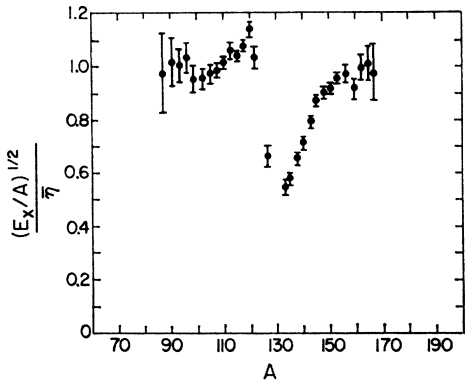

FIG. 20. The ratio of the square root of the excitation energy per particle to the average neutron kinetic energy, as a function of fragment mass. The ordinate was arbitrarily normalized to unity in the region of the light fragment.

particle, the above two quantities would be in a fixed ratio. We see that, in fact, if the ratio is normalized to about unity over the region of the light peak, a large difference is found in the mass range 130 through 140.

A more detailed examination of the relationship between excitation energy and $\bar{\eta}$ for four fragment masses is shown in Fig. 21. The value of $\bar{\eta}$ is plotted vs the square root of E_x/A. The value E_x was taken to be equal to E_n augmented by 2.5 MeV, an estimate of the contribution to the internal excitation energy per fragment associated with γ rays.[17] Again, if $\bar{\eta}$ could be taken as a measure of the temperature, and the temperatures were proportional to the square root of the excitation energy, such a plot should give a set of straight lines whose slopes would be related to the effective specific heats (a large slope implying a small specific heat). We note that the experimental points show considerable deviations from straight lines (some may be associated with poor statistics) but that the general trends again suggest very low effective specific heats in the region of masses around 133. Small specific heats are indeed to be expected for nuclei in the neighborhood of closed shells, the smaller number of effective degrees of freedom for such nuclei implying a higher energy per degree of freedom and thus a higher temperature for a given total excitation energy. This may again be illustrated with the help of Cameron's rule for level densities. The more lightly drawn curves in Fig. 22 show how different temperatures would be found in different nuclei excited to the same energy (this energy appears on a label to each curve on the left side of Fig. 22). We see that in the region of closed shells a given excitation produces unusually high temperatures. The sets of temperature curves in Fig. 22 were combined with the experimentally determined average excitation energies of different fragments, to produce the heavily drawn curves in Fig. 22 showing the temperature after the emission of one, two, three, or four neutrons by different fragments. (The observed average temperature of neutrons from a given fragment would correspond to some average over such a cascade.) We note that the sudden decrease in temperature due to the falling excitation in the region between masses 120 and 132 tends to be counteracted by the increasing temperature for a given excitation in the same region. The pattern of heavy curves in Fig. 22 may be compared with the experimental average energy $\bar{\eta}(A)$ in Fig. 8. Although definite conclusions cannot be drawn from this comparison, owing to the schematic nature of the calculations, it would appear that taking account of the smaller specific heats of closed-shell nuclei might tend to reproduce the general pattern of the experimental trends in $\bar{\eta}$, and that perhaps with some modifications in the level density formula, even quantitative agreement might be found. On the other hand, it should perhaps be pointed out that this way of reconciling the violent asymmetry of the saw-tooth curves for $\nu(A)$ and the approximately symmetric curves for $\bar{\eta}(A)$ would, at our present level of understanding, be in the nature of an accident, with the specific heat of closed-shell nuclei just low enough to bring the average temperature up to the same value as that of the much more highly excited nonmagic partner. A more direct way of interpreting the approximate equality of the temperatures of pairs of fragments (the approximate symmetry of the curves for $\bar{\eta}(A)$ in Fig. 6) would be to assume that the two undeformed fragments established their common temperature while in thermal contact at scission—the point of view of Newton,[13] Cameron,[14] and Newson,[15] mentioned earlier, which we believe to be difficult to reconcile with other aspects of fission. A clarification of the relations of the different

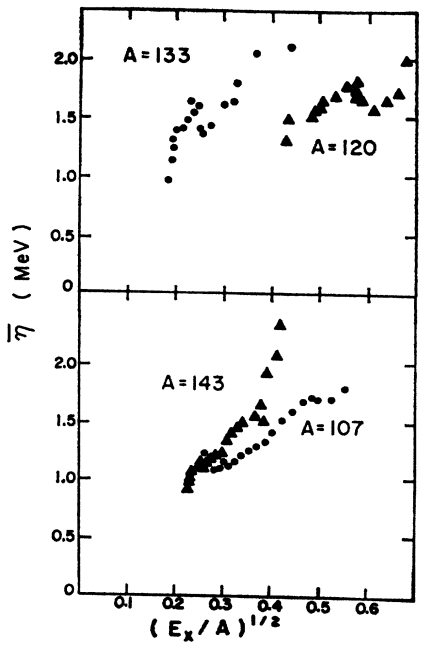

FIG. 21. The average neutron energy vs the square root of the excitation energy per particle, for four fragment masses.

[17] This implies that only about half of the observed γ-ray energy of 9 MeV per fission is associated with internal excitations of the fragments, as is suggested by an analysis of the competition between γ and neutron emission [see I. Halpern (fission), Ann. Rev. Nucl. Sci. 9, 245 (1959)]. The results are not significantly affected by this assumption.

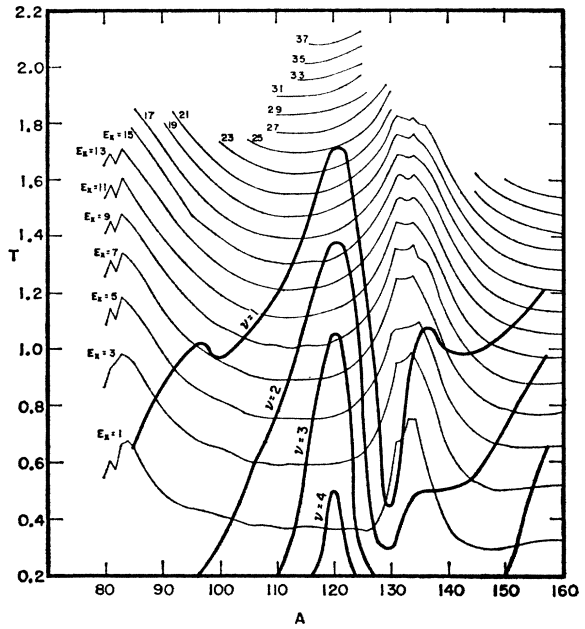

FIG. 22. Nuclear temperature T as a function of fragment mass and excitation energy E_x as calculated from the level-density prescription of Cameron. The heavy line gives the temperature after the emission of 1, 2, 3, or 4 neutrons, starting from the average value of the excitation energy.

hypotheses to the experimental data will require a more thoroughgoing analysis than we attempt here.

V. CONCLUSIONS

In conclusion, we would like to make two remarks concerning possible theoretical and experimental studies suggested by our experiment.

In the first place, we would like to stress that our principal objective has been to present the experimental results in a reasonably complete manner, and that a theoretical interpretation has not been aimed at.

When we do make comparisons with primitive theoretical estimates, it is more to bring out certain features of the data than to present a critical confrontation of theory and experiment. We hope that such a confrontation, dependent on the working out of an adequate theory, will be made in the future, and that the information contained in our experimental results will be exploited more fully than has been possible in this paper.

The second remark concerns the directions that we think future experiments on fission neutrons might profitably explore. It was in the nature of our experiment, aimed as it was at a relatively comprehensive study of the manifold neutron and fragment distributions and the resulting profusion of recorded events, that the analysis of the data came long after the actual measurements were over. As a result we are sometimes faced with the situation that an interesting effect suggested by the data—for example, the deviations from isotropic evaporation—remain poorly defined either on account of insufficient accuracy, or the absence of cross checks to eliminate alternative explanations. We feel that now, with the over-all nature of the neutron distributions established, it would be relatively easier to design more specialized experiments to study in detail and with high precision one or another of the interesting features suggested by our results. It is even reasonable to expect that the more decisive tests of our understanding of the process of nuclear fission and of the properties of fission fragments would come at this second, high-precision stage of the experimental studies of fission neutrons.

ACKNOWLEDGMENTS

We are especially grateful to Jean Rees and Arlene Fregulia for their help with calculations, data analysis, graphs, figures, and the final preparation of this paper. We wish to thank Llad Phillips and Ray Gatti for their help in several phases of the work described here. The help of Claudette Rugge with certain of the calculations and with computer programming is gratefully acknowledged. We are grateful to Professor Isadore Perlman for his continuous interest in and support of the work reported here.

We would like to thank Jim Terrell for comments concerning the manuscript.

APPENDICES

A. Formula for the nth Moment of the Center-of-Mass Neutron Spectrum

Using the relation between the laboratory-system velocity V and the center-of-mass velocity v, we have

$$v^2 = V^2 + V_f^2 - 2V_f V\cos\theta,$$

where V_f = fragment velocity. Using the Jacobian of the transformation from c.m. variables v, ψ to the lab variables V, θ,

$$J(v,\psi/V,\theta) = |V/v|,$$

we find the following expression for the nth moment of the c.m. velocity distribution (assumed isotropic):

$$\langle v^n\rangle = \sum_i \left[\frac{v^{n+1}/V^2}{\epsilon(V)}(V - V_f\cos\theta)\right]_i \Big/ \sum_i \left[\frac{v/V^2}{\epsilon(V)}(V - V_f\cos\theta)\right]_i \quad (n>0).$$

The sums are carried out, event by event, over all events for which

$$V - V_f\cos\theta \gtrless 0.$$

The denominator in the above expression may be defined as the zeroth moment $\langle v^0\rangle$. The number of neutrons with center-of-mass velocities greater than $V_f\sin\theta$ is then given by

$$\nu = 4\pi\langle v^0\rangle/\omega(R/2),$$

where ω is the solid angle subtended by counter, and R is the number of fissions recorded.

The number of neutrons with center-of-mass velocities less than $V_f \sin\theta$ (and which is therefore missed in the above expression) is very small if θ is small. For an evaporation spectrum with effective temperature T, the fraction missed is approximately $\eta_c^2/2T^2$, where η_c is the energy corresponding to $V_f \sin\theta$. In our case, with $\theta=11.25$ deg and $T=0.7$ MeV, this fraction is 0.16%. The effect on the higher moments is even smaller.

B. Corrections for Calculating Center-of-Mass Neutron Spectra

1. *Neutrons Coming from the Opposite Fragment*

For those data that rest solely upon the 11.25-deg results, the correction made necessary by the additional neutrons from the fragment traveling in the direction away from the detector may be made with the aid of ρ curves such as those in Fig. 22 of BTMS. In this way it was found that, for average fragments, ν_L and ν_H must be reduced by 0.3%. For nearly symmetrical fragments, the contribution of the heavy to the light is negligible, but the contribution of the light fragment to the heavy is $\approx 1\%$.

The influence on the average c.m. energy is similarly small, so the entire correction has been neglected for the small-angle data.

Although at first sight it might seem difficult, it is actually rather easy to correct the all-angle data for the loss of neutrons from the light-fragment into the heavy-fragment hemisphere and vice versa. Provided that the emission spectrum is isotropic and given by a superposition of evaporation spectra of the type

$$(\eta/T^2)\exp(-\eta/T),$$

it can be shown that the number "lost" into the backward hemisphere L is given by

$$L=\left(\frac{0.5226}{T}\right)^2\int_{V_f}^{\infty}(1-\cos\psi)v^3\exp\left(\frac{-0.5226v^2}{T}\right)dv.$$

The integration is most conveniently expressed in dimensionless form through the variable

$$t^2=2\eta_f/T=2(0.5226)V_f^2/T,$$

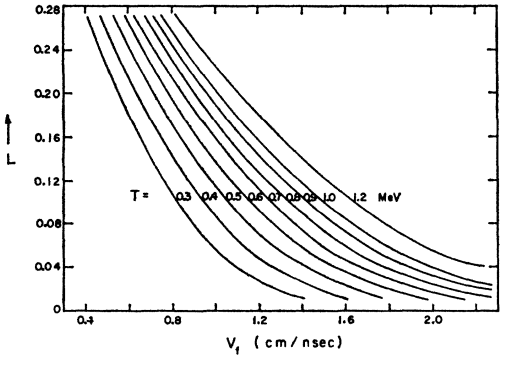

FIG. 23. Fraction of neutrons, L, going into the backward hemisphere in the laboratory system as a function of the temperature of the spectrum and the fragment velocity.

where η_f is the fragment energy; then

$$2L=(2\pi)^{1/2}\phi(t)-(\pi/2)^{1/2}t(0.5-\mathrm{erf}t),$$

where ϕ is the normalized Gaussian, and erf the error integral as defined in the *Handbook of Chemistry and Physics*. The result is shown in Fig. 23 for several values of the temperature. Thus, if the relation between fragment mass and velocity V_f is known, the observed neutron results ν may be corrected to ν' by using Fig. 23 and the relations

$$\nu_L'=[(1-L_H)\nu_L-L_H\nu_H]/(1-L_L-L_H),$$

and

$$\nu_H'=[(1-L_L)\nu_H-L_L\nu_L]/(1-L_L-L_H).$$

For Cf^{252}, L varies from a low of 0.03 at $A=80$ to a high of 0.24 at $A=160$.

The effect of neutron velocity resolution on ν is less than 4%, independent of A. The effect on $\bar{\eta}$ would be to reduce the average energy by about 3% over-all.

2. *Correction for Zero Efficiency at Low Laboratory-System Velocities*

This correction is unnecessary for the 11.25-deg data, since at no time are velocities less than 1 cm/nsec used; however, it is quite important to the all-angle data. Its presence shows up in ν simply as a fractional loss of events that is nearly independent of the velocity of the fragments. Thus the number of neutrons found with velocities greater than the cutoff velocity of 1 cm/nsec was 3.35, to be compared with the known total of 3.82. Accordingly, in plotting the squares in Fig. 8, all values for ν were multiplied by the factor $3.82/3.25=1.14$ to force the total number of neutrons observed to be equal to 3.82. The correction is rather large for the average energy, entailing a reduction by as much as 50%. These results have not been presented because of the difficulty in estimating an accurate correction of this magnitude.

C. Corrections for Dispersion

In almost all cases, the most serious corrections were those of mass or energy resolution arising from the spread in the measured fragment-flight times. The indicated variances of the mass distribution σ_A^2 and the total kinetic energy distribution σ_K^2 were 7.0 (mass units)^2 and 83 (MeV)^2, respectively, corresponding to widths (FWHM) of 6.2 mass units and 21.5 MeV. Although a mass resolution of 6.2 units is too large to reveal any appreciable fine structure resulting from a single mass, it is nevertheless small compared with the width 15.2 of the intrinsic mass peak.[18] On the other hand, the intrinsic width of the total kinetic energy distribution is 24.6 MeV,[14] and the resolution width of 21.5 MeV is anything but small. We should therefore not expect to see any fine-structure effects whatever in the total kinetic energy.

[18] J. C. D. Milton and J. S. Fraser, Phys. Rev. **111**, 887 (1958).

Because of the qualitative difference in the size of the mass and energy resolutions, we adopted a different procedure in correcting for them. In the case of the mass, the procedure used was one suggested by Terrell.[5] Provided that over the range of the resolution function the observed distribution is everywhere adequately approximated by a polynomial of degree 3 or less, it can be shown for symmetrical resolution functions that the true distribution may be found from the observed G by the fold

$$g(x)=\int G(x-y)u(y)dy,$$

where $u(y)$ is an undispersing function. The only condition that must be satisfied by the function u is that it have a variance equal in size, but opposite in sign, to the resolution function.

The method outlined above is extremely neat and easy to use when it is applicable. However, it will lead to false results if the cubic expansion is insufficient, and this will often be the case when the resolution width is comparable to the intrinsic width. In fact, this was the case of the energy resolution in our experiment. Of course, it is possible to allow for an expansion up to the fifth degree by including the fourth moments, but these are generally not well known. Although general methods are available involving Taylor's expansion, and consequently requiring the evaluation of the first and, perhaps, second derivatives of the experimental distribution function, the total kinetic energy distribution is sufficiently Gaussian that we may apply a useful but special method. If the resolution function is also Gaussian with a variance σ^2, while the variance of the *observed* distributions is s^2, then any linear function of the independent variable x given by $y=a+bx$ will be observed as a straight line with the equation

$$y_{\text{obs}}=a+bx(1-\sigma^2/s^2),$$

where the origin has been taken at the position of the mean. In particular, the "calibration" equation $y=x$ will have its slope reduced to $(1-\sigma^2/s^2)$. Thus, for Gaussian intrinsic distribution and resolution functions, any observed function of x may be resolution corrected simply by plotting the value at the corrected x point.

PHYSICAL REVIEW VOLUME 129, NUMBER 5 1 MARCH 1963

Lifetime Determination of the 2+ and 4+ Rotational Levels in Gd^{154} and the Effect of Rotation-Vibration Interaction

J. BURDE, M. RAKAVY, AND G. RAKAVY
Department of Physics, The Hebrew University, Jerusalem, Israel
(Received 8 October 1962)

The lifetimes of the 2+ and 4+ rotational levels of Gd^{154} were determined by coincidence measurements between the beta spectrum of Eu^{154} and the conversion lines de-exciting the levels under investigation, utilizing a double-lens coincidence spectrometer. The measurements were carried out using the self-comparison method and a time-to-amplitude converter. The mean lifetimes of the 371- and the 123-keV levels were found to be $(5.6\pm0.7)\times10^{-11}$ sec and $(1.67\pm0.07)\times10^{-9}$ sec, respectively. The measured ratio for the reduced transition probabilities, $B(E2;4+\rightarrow2+)/B(E2;2+\rightarrow0+)=1.77\pm0.25$, deviates from the value 1.43 predicted by the strict rotational model. The effect of rotation-vibration interaction on the transition probability ratios within a rotational band is discussed. These ratios are related uniquely to the distortion of the energy spacings. In the case of the ground-state band of Gd^{154}, theory thus predicts $B(E2;4+\rightarrow2+)/B(E2;2+\rightarrow0+)=1.62$ in agreement with experiment.

INTRODUCTION

RECENTLY, with the improvement of lifetime measurement technique, some interest has been revived in lifetime determination of the two lowest excited states of even-even nuclei for strongly distorted nuclei. The strong-coupling model predicts a unique ratio between the reduced probabilities for transitions starting from the second 4+ excited state to the transitions from the first 2+ level. This theoretical ratio has been consistent within experimental error with values deduced from lifetime measurements in nuclei having a well-developed rotational spectra.[1-4] Very recent results for Dy^{160}, however, as discussed in the last section of this article, seem to indicate a discrepancy with theory.

In Os^{190}, where the energy interval rule is not strictly obeyed, it has been found[1] that the ratio of the transition probabilities is appreciably lower. This nucleus lies at the upper edge of a region of strongly distorted nuclei.

It was of great interest to find out this ratio in a nucleus lying at the lower side of this strong coupling region.

An abrupt transition in the properties of the nuclei occurs as the neutron number changes from 88 to 90. Sm^{152} and Gd^{154}, each of them having 90 neutrons, are at the verge of a region of strongly deformed nuclei. However, these nuclei displaying a considerable deviation from the rotational energy interval rule may still

[1] G. Scharff-Goldhaber, D. E. Alburger, G. Harbottle, and M. McKeown, Phys. Rev. **111**, 913 (1958).
[2] S. Ofer, Phys. Rev. **115**, 412 (1959).
[3] J. Burde and M. Rakavy, Nucl. Phys. **28**, 172 (1961).
[4] A. C. Li and A. Schwarzchild, Bull. Am. Phys. Soc. **7**, 359 (1962).